

Quantum Interference of Tunably Indistinguishable Photons from Remote Organic Molecules

R. Lettow¹, Y. L. A. Rezus¹, A. Renn¹, G.

Zumofen¹, E. Ikonen², S. Gotzinger¹, V. Sandoghdar¹

¹Laboratory of Physical Chemistry and optETH,

ETH Zurich, CH-8093 Zurich, Switzerland

²Metrology Research Institute, Helsinki University of Technology (TKK) and

Centre for Metrology and Accreditation (Mikes),

P.O. Box 3000, FI-02015 TKK, Finland

Abstract

We demonstrate two-photon interference using two remote single molecules as bright solid-state sources of indistinguishable photons. By varying the transition frequency and spectral width of one molecule, we tune and explore the effect of photon distinguishability. We discuss future improvements on the brightness of single-photon beams, their integration by large numbers on chips, and the extension of our experimental scheme to coupling and entanglement of distant molecules.

PACS numbers: 42.50.Ar, 42.50.Dv, 03.67.Lx, 42.50.Lc

Recent developments in quantum engineering have redrawn the attention of scientists to the phenomenon of interference between single photons [1, 2, 3, 4, 5, 6, 7] for its potential in applications such as entanglement generation [8] and optical quantum computing [9, 10]. In a two-photon quantum interference (TPQI) experiment indistinguishable single photons from two independent beams enter the two input ports of a 50-50 beam splitter and leave together in one of the two output ports [11]. Although the pioneering work on this topic used photon pairs created in parametric down conversion [12], ideally, it is desirable to use a large number of bright independent sources of Fourier-limited photons. It turns out that single quantum emitters are predestined for this task because they are intrinsically small and can emit lifetime-limited photons one at a time [13]. Indeed, atoms and ions in vacuum chambers have been successfully used in the context of TPQI interference measurements [2, 4, 5]. However, atom reloading time, difficulties in efficient light collection, and scaling to large numbers of emitters pose major challenges to various realizations. Solid-state emitters such as semiconductor quantum dots, color centers, and molecules are scalable on chips, can have large emission rates, and lend themselves to highly efficient collection schemes [14]. However, they face the main hurdles of spectral dephasing and inhomogeneity, which make it difficult to find independent emitters that generate indistinguishable photons. In this work, we show that organic molecules embedded in organic matrices master all these challenges and discuss the conditions for tolerating deviations from the ideal case.

The organic dye molecules in this study were dibenzanthanthrene (DBATT) embedded in *n*-tetradecane at a concentration of about 10^{-6} M. As illustrated in Fig. 1a and described in detail in Ref. [15], we used separate microscopes and samples to extract indistinguishable photons on the zero-phonon lines (ZPLs) of two remote molecules. At cryogenic temperatures ($T < 2$ K), DBATT displays a sharp lifetime-limited ZPL (~ 17 MHz) between the ground vibrational level of the electronic ground state $S_{0,v=0}$ and the ground vibrational level of the electronic excited state $S_{1,v=0}$ at 589 nm (see Fig. 1b) [16]. We used a narrow-band (< 1 MHz) dye laser to address molecules across the inhomogeneous spectral distribution of the sample (~ 2 THz) [17]. As the frequency of the laser was scanned, ZPLs of individual molecules were excited selectively, and we recorded the Stokes-shifted fluorescence on the $S_{1,v=0} \rightarrow S_{0,v \neq 0}$ transitions (see Fig. 1b) to detect each molecule [18]. To obtain the same ZPL frequency for two molecules in the two samples, we tuned the resonance of one molecule by applying a voltage to the gold microelectrodes fabricated on its substrate (see Fig. 1c).

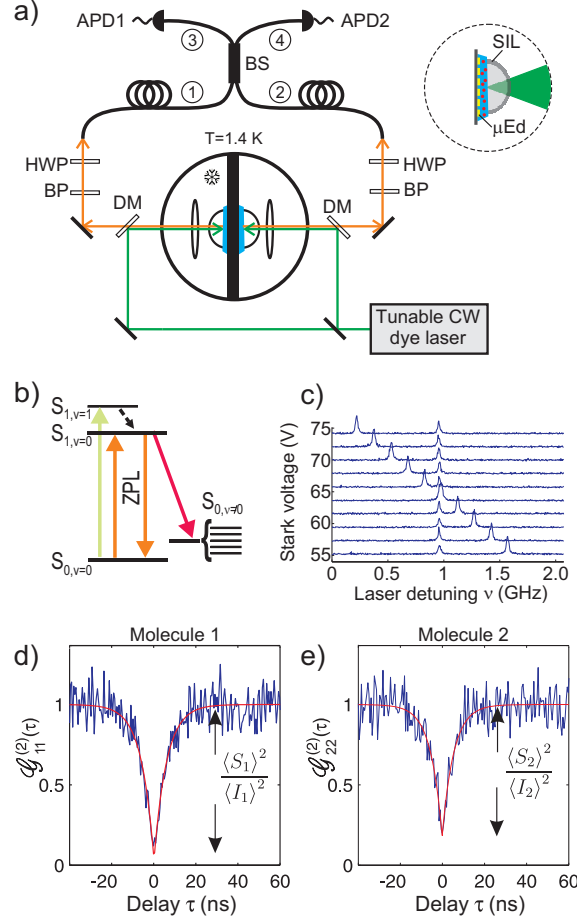


FIG. 1: a) Schematic diagram of the optical setup. DM, dichroic mirror; BS, beam splitter; BP, bandpass filter; HWP, half-wave plate; APD, avalanche photodiode; SIL, solid-immersion lens; Ed, gold microelectrodes. b) Energy level diagram of a DBATT molecule. c) Fluorescence excitation spectra of two selected molecules as a function of the voltage on the microelectrodes of one sample. This Stark effect was linear and well described by the relation $\nu = 50 \text{ (V}^{-1} \text{ 63)}$ (with ν in MHz and V in Volts). d, e) Intensity autocorrelation functions of the two molecules. See text for the details of the theoretical fit.

Once we had prepared two molecules with identical ZPLs, we generated Fourier-limited single photons from them by tuning the dye laser frequency to the transition between the ground state and the first vibrational level of the electronic excited state ($S_{1,v=1}$). We found that despite having the same ZPL, the $S_{0,v=0} \rightarrow S_{1,v=1}$ transition frequencies were typically not the same for the two selected molecules. Nevertheless, these transitions overlapped within their linewidths of about 30 GHz [15], allowing us to excite the two molecules equally strongly by a suitable adjustment of the laser frequency. The $S_{1,v=1}$ rapidly relaxes to the $S_{1,v=0}$ state which has a lifetime of 9.5 ns determined by a radiative decay to $S_{0,v=0}$ (ZPL)

or $S_{0,\nu \neq 0}$ with a branching ratio of about 0.5 (see Fig. 1b). The emission on the ZPL with a coherence length of about 3 m yielded up to one million counts on the detector after passing a bandpass filter to reject the excitation light and the Stokes-shifted fluorescence [15]. It is worth emphasizing that the transition dipole associated with the ZPL has a well-defined orientation with respect to the backbone of the molecular structure, leading to a linearly polarized emission.

To realize an arrangement for a TPQI measurement, the ZPL emissions of the two molecules were focussed into the two arms of a single-mode polarization-maintaining fiber beam splitter, which conveniently ensured spatial mode matching of the two beams (see Fig. 1a). Two halfwave plates were used to align the input polarizations. The outputs of this device were directed to two avalanche photodiodes (APDs) connected to a time-to-amplitude converter that functioned in a start-stop configuration and allowed us to record intensity correlations with a time resolution of 800 ps. In a first step, we always verified that each beam consisted of single photons by recording its intensity autocorrelation function $g^{(2)}(\tau)$ separately when the other fiber input was blocked. Figures 1d,e display strong photon

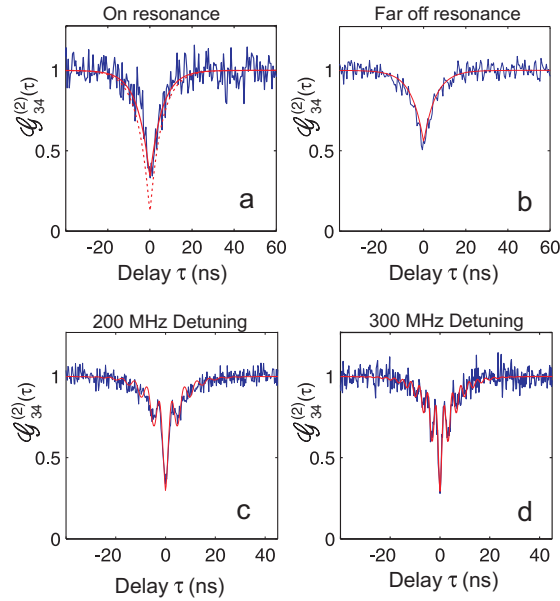


FIG. 2: a) Intensity cross correlation function of photons with the same ZPL frequency (on-resonant) exiting the output ports of the beam splitter. b) Same as (a) if the ZPL of one molecule is frequency detuned by about 5 GHz (far off resonant). c,d) Same as (a) if the two emitters are frequency detuned by 200 MHz and 300 MHz, respectively. The red curves are calculations based on Eqn. (1) with $\eta = 0.5$ (solid) and $\eta = 1$ (dashed), respectively.

antibunching at zero time delay for two molecules ($i=1,2$) from the two samples. In the ideal case, one expects $g_{ii}^{(2)}(0) = 0$ [19]. If the single-photon intensity (S_i) of each molecule is accompanied by an uncorrelated background (B_i), the overall detected intensity $I_i = S_i + B_i$ satisfies $\mathcal{G}_{ii}^{(2)}(\tau) = 1 + \frac{hS_i i^2}{hI_i i^2} [g_{ii}^{(2)}(\tau) - 1]$. In what follows, we use the calligraphic notation $\mathcal{G}(\tau)$ to denote a measurement in the presence of background and reserve $g(\tau)$ for the ideal correlation functions. The measured autocorrelation functions $\mathcal{G}_{ii}^{(2)}(0) = 1 - \frac{hS_i i^2}{hI_i i^2}$ shown in Figs. 1d,e reveal that $\frac{hS_i i}{hI_i i} \approx 90\%$. In our experiment, the residual background stemmed from neighboring nonresonant molecules in the excitation spot, which can be eliminated by reducing the DBATT concentration during sample preparation.

For a beam consisting of single photons from two different molecules, $g^{(2)}(0)$ is reduced to 0.5 because the detection of a photon from one molecule does not impede detecting a second one from the other molecule [19]. The fascinating feature of a TPQI experiment is that even photons from two independent emitters can yield a perfect anticorrelation. Here, two photons that are indistinguishable in frequency, linewidth, spatial mode, and polarization enter the two input arms of a beam splitter (labeled 1 and 2) and coalesce in one of the output ports (labeled 3 and 4) so that the probability of simultaneously detecting one photon in each arm vanishes at zero time delay [20]. The theoretical expression for the intensity cross correlation function of the two outgoing modes of the beam splitter reads [see Supplementary Material],

$$\begin{aligned} \mathcal{G}_{34}^{(2)}(\tau) &= c_1^2 \mathcal{G}_{11}^{(2)}(\tau) + c_2^2 \mathcal{G}_{22}^{(2)}(\tau) \\ &+ 2c_1 c_2 \left[1 - \frac{hS_1 i hS_2 i}{hI_1 i hI_2 i} g_{11}^{(1)}(\tau) g_{22}^{(1)}(\tau) \right] \cos(\Delta \tau) \end{aligned} \quad (1)$$

where $c_i = I_i/(I_1 + I_2)$. The first and second terms represent the intensity autocorrelations of the individual sources as measured experimentally and presented in Figs. 1d and 1e, whereas the term in brackets originates from the mixed products of the two input intensities at frequency detuning Δ . For a quantum emitter i , the intensity (second order) and field (first order) autocorrelation functions are related according to $g_{ii}^{(2)}(\tau) = 1 - [g_{ii}^{(1)}(\tau)]^2$ where $g_{ii}^{(1)}(\tau) = e^{-i\Delta \tau} e^{-\gamma|\tau|/2}$ and γ is the homogeneous linewidth of the emitter [19]. Thus, the measurements of $\mathcal{G}_{ii}^{(2)}$ determine both the ratios $\frac{hS_i i}{hI_i i}$ and $g_{ii}^{(1)}$, therefore fully characterizing $\mathcal{G}_{34}^{(2)}(\tau)$. In practice, the visibility of the two-photon interference could be reduced by fac-

tors other than the background light. We have, therefore, included the phenomenological parameter $\theta = 1$ in Eqn. (1) to account for this effect.

The blue trace in Fig. 2a displays $\mathcal{G}_{34}^{(2)}(\tau)$ for the two output ports of the beam splitter when the inputs were photons emitted by the same two molecules presented in Figs. 1d,e. The fact that $\mathcal{G}_{34}^{(2)}(0) < 0.5$ is a clear proof of a quantum interference and has its origin in the corpuscular nature of single-emitter radiation [11, 20]. The red curve shows a very good agreement with the predictions of Eqn. (1) based on the data from the experimental measurements of $\mathcal{G}_{ii}^{(2)}(\tau)$ and with the assumption that $\theta = 0.5$. The origin of the contrast reduction was due to polarization ellipticities caused by a number of depolarizing elements such as dielectric mirrors and cryostat windows. For comparison, the dashed red curve displays the prediction of the calculations for $\theta = 1$.

To examine the impact of photon distinguishability on the cross correlation function, we exploited the frequency tunability of our emitters and changed the frequency of one molecule. First, we explored the case of far-off detuning by setting $\Delta = 2 \times 5 \text{ GHz}$. Figure 2b confirms that in this case, we obtained $\mathcal{G}_{34}^{(2)}(0) \approx 0.5$. The red curve shows a very good agreement with the outcome of calculation with no free parameters and assuming $\theta = 0$. The latter condition is justified by the fact that for photons with a large frequency difference, the term proportional to the cosine in Eqn. (1) is washed out due to the limited time resolution of our detectors. At the same time, this term suggests that a frequency mismatch between the two emitters should introduce a time-dependent beat signal in the coincidence counts [2]. Figures 2c and d display the measured two-photon interference signal when the ZPL of one molecule was detuned by $\Delta = 2 \times 200 \text{ MHz}$ and $\Delta = 2 \times 300 \text{ MHz}$, respectively. The solid red curves show that again calculations based on $\theta = 0.5$ provide excellent agreement with the experimental findings. It is noteworthy that although the two photons are clearly distinguishable in frequency, we still find $\mathcal{G}_{34}^{(2)}(0) < 0.5$. Quantum beat signals shown in Figs. 2c,d were observed for the interference of delayed photons from a single atom [2], but to our knowledge, this is the first demonstration for photons from independent sources.

A key asset of organic molecules is that they routinely exhibit resonances with natural linewidth [13]. Although other solid-state systems such as semiconductor quantum dots and color centers can, in principle, also reach this level of coherence, their performance has been critically dependent on the sample quality and reports of Fourier-limited emission from these systems are still missing. Dephasing and spectral diffusion processes in solid-state emitters

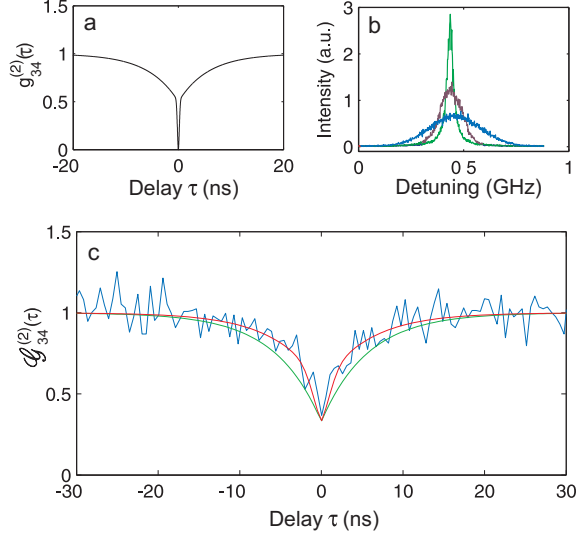


FIG. 3: a) Theoretical prediction of the $g_{34}^{(2)}$ function when one molecule is broadened by about 120 times the natural linewidth γ_0 . b) Fluorescence excitation spectra of the ZPL for different noise amplitudes applied to the electrode. FWHM = 30 MHz (blue), 120 (green), and 300 (red). c) Experimental measurement of the two-photon interference where the ZPL of one molecule was artificially broadened. The red curve is the prediction of Eqn. (1) for $\gamma = 0.5$ and the green curve displays the data from Fig. 2a.

result in fast variations of the emitter resonance frequency and therefore fluctuations of δ in Eqn. (1). As an example, Fig. 3a shows the theoretical predictions if one of the ZPL of one molecule were broadened to a full width at half maximum (FWHM) of 2 GHz. Although we still find $g_{34}^{(2)}(0) = 0$, a finite detector time resolution of the order of 1 ns would wash out the contrast. In order to explore this experimentally, we artificially broadened the ZPL of one of the two molecules by applying quasi-white noise to its sample microelectrodes. Figure 3b illustrates the resulting ZPL with FWHM = 300 MHz ($\approx 18\gamma_0$) at the maximum amplitude of the applied noise. We note in passing that the line profiles are no longer Lorentzian because of the limited modulation bandwidth of 1 MHz that was used in the Stark broadening process. The blue trace in Fig. 3c displays the resulting $g_{34}^{(2)}(\tau)$ measurement, and the red solid curve shows the prediction of Eqn. (1) with $\gamma = 0.5$. As compared to the green curve which recasts the data of Fig. 2a, the TPQI dip narrows but the contrast reduction is not substantial because as in the case presented in Fig. 2d, the response of our detectors has been sufficiently fast for resolving the features of $g_{34}^{(2)}$. In summary, current photodetectors allow a considerable deviation of the spectral coherence from the ideal Fourier-limited condition without compromising the signature of the two-photon interference. Nevertheless, it has to

be born in mind that any dephasing or spectral diffusion process reduces the probability of two-photon coalescence after the beam splitter because it lowers the coherence time of the photons ($l = \tau$) with respect to their radiative lifetime ($l = \tau_0$).

Other important and desirable features of single-photon sources for exploiting quantum interference measurements are high emission rates, large collection efficiency, and integration of a large number of sources. Solid-state systems and in particular organic molecules promise to address all of these criteria at the same time. By excitation to the $S_{1,v=1}$ state via short pulses, DBATT can emit one photon per excited-state lifetime of 9.5 ns, thus reaching a rate of few tens of MHz [21]. For an emitter at the interface of a medium with a high refractive index (see Fig. 1a), collection efficiencies beyond 90% can be achieved by optimizing the choices of the solid-immersion lens and the numerical aperture of the collecting lens [22]. A collection efficiency of about 50% and an overall detection efficiency (filters, detector quantum efficiency, etc.) of 10% would yield more than $10^7 (0.5 \cdot 0.1)^2 > 10000$ coincidences per second. Furthermore, one can integrate a large number of small solid-immersion lenses and independently addressable microelectrodes on the sample to extract many single photon beams simultaneously [21].

Manipulation of Fourier-limited photons emitted by organic molecules paves the way towards a number of interesting experiments. First, our experimental setup can be readily used to perform spectroscopy on one molecule with tunable single photons emitted by the second molecule [23]. Furthermore, the two-photon interference arrangement gives access to a conditional entanglement [24] of distant molecules. Although this entanglement only lasts during the lifetime of the electronic state (about ten nanoseconds), application of ultrafast pulses can allow a large number of coherent qubit rotations [25]. Moreover, one can envision replacing free-space photon channels used in our current experiment with on-chip dielectric waveguides [26]. Such a photonic circuit would offer a "hard-wire" compact network of many individually-addressable single-photon sources for complex quantum information processing tasks.

We thank M. Pototschnig and J. Hwang for experimental help and R. Pfaff and V. Ahtee for contribution to the initial phase of the experiment. This work was supported by the Swiss National Science Foundation (SNF) and ETH Zurich (Fellowship to Y.R. and the Q-SIT project grant Nr. PP-01-07-02). E.I. acknowledges the warm hospitality during his numerous visits at ETH and grant Nr. 129971 from the Academy of Finland.

-
- [1] C . Santori, D . Fattal, J . Vuckovic, G . S . Solomon, and Y . Yamamoto, *Nature* 419, 594 (2002).
 - [2] T . Legero, T . Wilk, M . Hennrich, G . Rempe, and A . Kuhn, *Phys. Rev. Lett.* 93, 070503 (2004).
 - [3] A . Kiraz, et al, *Phys. Rev. Lett.* 94, 223602 (2005).
 - [4] J . Beugnon, et al, *Nature* 440, 779 (2006).
 - [5] P . Mounz, et al, *Nat. Phys* 3, 538 (2007).
 - [6] K . Sanaka, A . Pawlis, T . D . Ladd, K . Lischka, and Y . Yamamoto, *Phys. Rev. Lett.* 103, 053601 (2009).
 - [7] A . J . Bennett, R . B . Patel, C . A . Nicoll, D . A . Ritchie, and A . J . Shields, *Nature Phys.* 5, 715 (2009).
 - [8] Z . Y . Ou and L . Mandel, *Phys. Rev. Lett.* 61, 50 (1988).
 - [9] E . Knill, R . Laamme, and G . J . Milburn, *Nature* 409, 46 (2001).
 - [10] J . L . O'Brien, G . J . Pryde, A . G . White, T . C . Ralph, and D . Branning, *Nature* 426, 264 (2003).
 - [11] H . Paul, *Rev. Mod. Phys.* 58, 209 (1986).
 - [12] C . K . Hong, Z . Y . Ou, and L . Mandel, *Phys. Rev. Lett.* 59, 2044 (1987).
 - [13] B . Lounis and M . Orrit, *Rep. Prog. Phys.* 68, 1129 (2005).
 - [14] W . Barnes, et al, *Eur. Phys. J. D* 18, 197 (2002).
 - [15] R . Lettow, et al, *Opt. Express* 15, 15842 (2007).
 - [16] C . Brunel, B . Lounis, P . Tamarat, and M . Orrit, *Phys. Rev. Lett.* 83, 2722 (1999).
 - [17] W . E . Moerner and L . Kador, *Phys. Rev. Lett.* 62, 2535 (1989).
 - [18] M . Orrit and J . Bernard, *Phys. Rev. Lett.* 65, 2716 (1990).
 - [19] R . Loudon, *Quantum Theory of Light* (Oxford University Press, 2000).
 - [20] T . Legero, T . Wilk, A . Kuhn, and G . Rempe, *Adv. Atom. Mol. Opt. Phys.* 53, 253 (2006).
 - [21] V . Ahtee, et al, *J. Mod. Opt.* 56, 161 (2009).
 - [22] K . Koyama, M . Yoshita, M . Baba, T . Suemoto, and H . Akiyama, *Appl. Phys. Lett.* 75, 1667 (1999).
 - [23] G . Wrigge, I . Gerhardt, J . Hwang, G . Zumofen, and V . Sandoghdar, *Nature Phys.* 4, 60 (2008).
 - [24] D . L . Moehering, et al, *Nature* 449, 68 (2007).

- [25] I. Gerhardt, et al, Phys. Rev. A . 79, 011402 (R) (2009).
- [26] Q. Quan, I. Bulu, and M. Loncar, Phys. Rev. A 80, 011810 (R) (2009).